

## RESEARCH MANUSCRIPT

### Fractal graphs by iterated substitution

Henry Segerman\*

*Department of Mathematics and Statistics, University of Melbourne, VIC 3010, Australia*

*(Received 00 Month 200x; final version received 00 Month 200x)*

Space filling curves are well known examples from analysis, which can be seen as examples of fractals produced by iterated substitution. Steps in the construction of three dimensional space filling curves have also been popular subjects of mathematical sculpture, but suffer from potential structural problems due to the low levels of interconnectivity inherent in a curve. We introduce a generalisation of the construction of space filling curves to constructions of fractal graphs by iterated substitution. These follow the same kind of substitution rules but allow vertex degrees to be greater than two. We also introduce the use of the Cheeger constant as a way to evaluate the structural strength of a sculpture based on a graph, from a purely graph theoretic point of view.

**Keywords:** space filling curves; fractal; iterated substitution; graph theory; Cheeger constant; mathematical sculpture

*AMS Subject Classification:* 05C62

This is a preprint of an article whose final and definitive form has been published in the Journal of Mathematics and the Arts, ©2011 Taylor & Francis; the Journal of Mathematics and the Arts is available online at: <http://www.informaworld.com/smpp/>

#### 1. Introduction

Steps in the constructions of 3-dimensional space filling curves have been used as the subject of mathematical sculptures by a number of artists, for example Séquin in bronze [9], Goodman-Strauss using metal plumbing supplies (a sculpture constructed on site at the Gathering 4 Gardner 9 Conference in Atlanta, Georgia on 27<sup>th</sup> March 2010), and Muller has proposed using such a curve as a radiator [7].

A curve in a space can be thought of as a continuous function from the unit interval to the space, and a space filling curve is a curve whose image fills the entire space. Our space will usually be the unit square or unit cube. Space filling curves are generally fractal objects, constructed via a limiting process. That is, one constructs a sequence of piecewise linear curves with the property that subsequent curves pass more and more densely through the space, and the limiting fractal object fills the space. By “steps in the construction of the space filling curve” we mean the members of such a sequence. See Figure 1 for an example showing three steps in the construction of the (2-dimensional) Hilbert curve.

For aesthetic reasons artists have generally restricted themselves to constructions of space filling curves such that at each step the curve does not self-intersect (as in Figure 1). As a result, for sculptures of 3-dimensional examples the materials used must be strong enough to overcome

---

\*Email: [segerman@unimelb.edu.au](mailto:segerman@unimelb.edu.au)

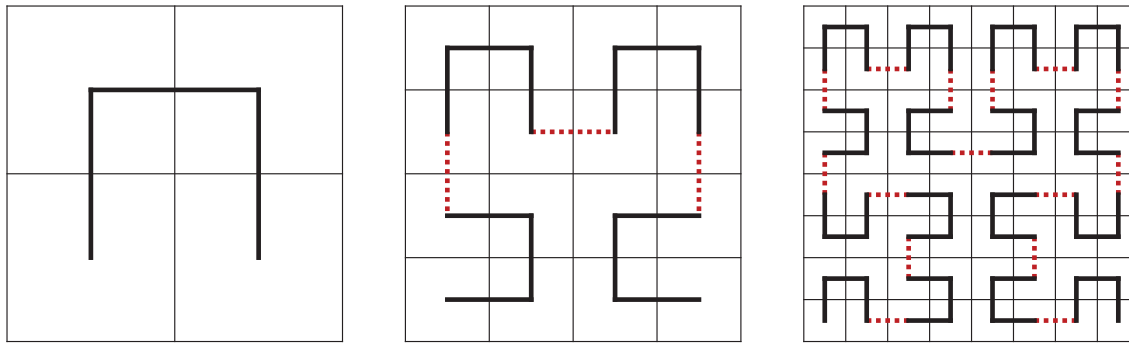


Figure 1. Three steps in the construction of the Hilbert curve.

potential structural problems: The artefact is a single very long curve, and the concept of the sculpture does not allow for supports. The problems only increase if we try to represent further, more intricate steps in the constructions. In fact, each of the sculptures listed above is of the third step in a construction of a 3-dimensional Hilbert curve (where the first step is a curve on the edges of a single cube). To the author's knowledge, no one has attempted to construct a physical sculpture of the fourth step (although there may be aesthetic as well as practical reasons for stopping at the third step). In Figure 2 we see another sculpture of the third step in the construction of a 3-dimensional Hilbert curve, by the author. The physical object is very flexible, and at least if we were to use the same materials, it seems unlikely that the fourth step would be able to support its own weight without bending to rest on itself.

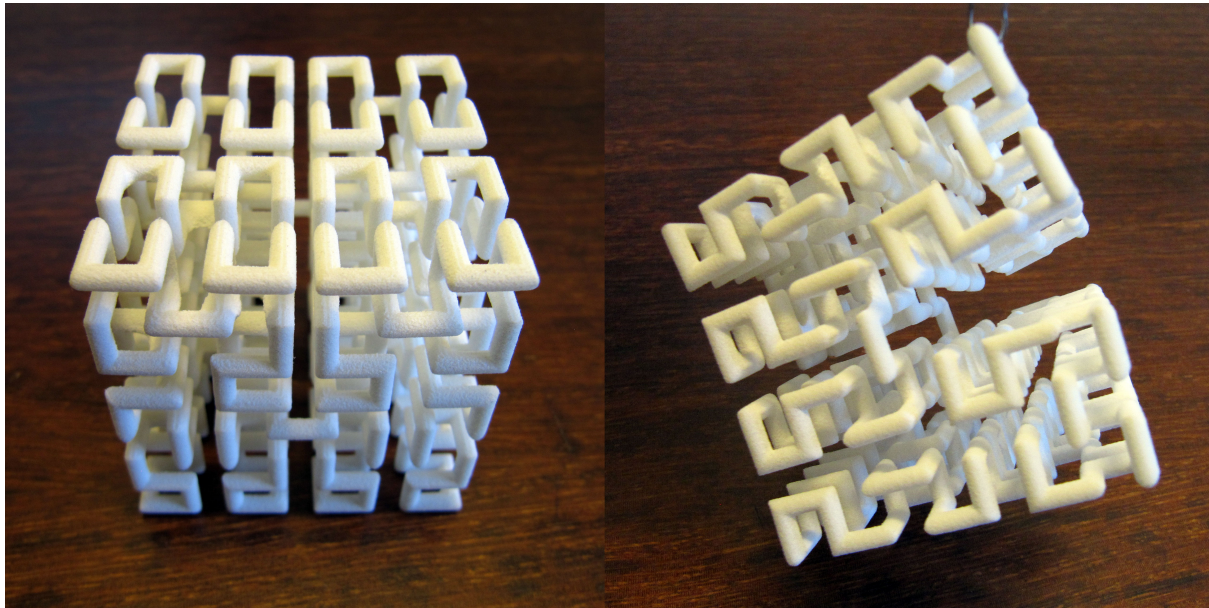


Figure 2. On the left a sculpture by the author showing the third step in the construction of a 3-dimensional Hilbert cube. On the right: when stressed (here by picking the sculpture up by a corner) it deforms significantly. This and other sculptures in this paper were realised in PA 2200 plastic using selective laser sintering by Shapeways.com.

In light of these issues we propose investigating more highly connected graphs, which retain the interesting self-similarity or limiting space filling properties but should be more robust as physical objects and allow us to build more intricate sculptures.

We would also like to have some form of quantitative measure of physical robustness, in order to determine if our more highly connected graphs are in fact more robust. The strength and

durability of physical constructions are of huge importance in engineering, and are studied in the field of structural analysis, generally using computer aided numerical approximation techniques. However, measures of structural integrity based on these techniques are in general not amenable to analysis using pure mathematical arguments. Instead in this paper we propose an alternative, in some ways simpler measure of structural integrity, the Cheeger constant, which measures to what extent there are “bottlenecks” in a graph. The intuition comes from viewing a graph as a network, say of roads in a city. A bottleneck occurs when there are only a small number of edges in the graph connecting two large parts of the graph. In the analogy with roads in a city, the bottleneck could be the small number of bridges connecting the two halves of the city across a river.

**Definition 1.1** For a graph  $G$  with vertex set  $V$  and edge set  $E$ , and for a collection of vertices  $A$ , let  $\partial A$  denote the collection of all edges with one vertex in  $A$  and the other vertex in  $V \setminus A$ . The **Cheeger constant** of a graph  $G$  is defined by:

$$h(G) := \min \left\{ \frac{|\partial A|}{|A|} \mid A \subset V, 0 < |A| \leq \frac{|V|}{2} \right\}$$

The Cheeger constant is simple enough that it is possible to analyse with mathematical arguments and is used in many areas, including the study of computer networks and in low-dimensional topology. See [6].

**Example 1.2** For a graph in which every vertex has degree 2 (in this paper we will call a graph of this form a **closed curve**), we can minimise the value  $\frac{|\partial A|}{|A|}$  by choosing  $A$  to be some connected half of the closed curve, and so the Cheeger constant is  $\frac{4}{|V|}$  (if  $|V|$  is even) or  $\frac{4}{|V|-1}$  (if  $|V|$  is odd). A graph in which every vertex has degree 2 apart from two vertices with degree 1 (the “endpoints”) has Cheeger constant  $\frac{2}{|V|}$  (if  $|V|$  is even) or  $\frac{2}{|V|-1}$  (if  $|V|$  is odd).

## 2. The Cheeger constant and structural integrity

We believe that the Cheeger constant is of relevance to physical structures based on graphs for the following reason: If two large connected parts of a graph are connected to each other by only a few edges (i.e. we have a bottleneck), then those edges will be potential weak points for the physical structure.

To have a weak point in a graph, it is important both that there are only a few edges connecting two parts of the graph, but also that those two parts are large. In contrast, the **edge connectivity** of a graph is the minimum number of edges that need to be removed to disconnect the graph, and can be written as:

$$\lambda(G) := \min \{ |\partial A| \mid A \subset V, \emptyset \neq A \neq V \}$$

The edge connectivity of a graph would not be a good measure of the robustness of a physical representation of a graph. For the kinds of graph one might want to build a physical model of (e.g. some subset of a cubic lattice), the  $A$  achieving the minimum in the above definition could be just a single vertex (connected to the rest of the graph by perhaps 3 or 4 edges). While it is true that putting a large amount of stress on just those edges would cause damage to the structure, it is unlikely that a sculpture would be subject to such stresses, rather than forces affecting a larger part of the graph all at once. In particular, if the stresses are due to the effect of gravity on the mass of the sculpture itself, then the stress on a “bottleneck” collection of edges dividing the sculpture into two parts will be directly related to the size of the part that is

supported only by those edges (i.e. not attached to the ground).

Thus it makes sense to weight the expression we are minimising by the sizes of the parts involved. We might assume that we would arrange the sculpture so that it is the larger of the two parts of the graph divided by a bottleneck that is attached to the ground, and that the forces act on the smaller part. Therefore we should weight the expression by the size of the smaller of the two parts, which leads us to the Cheeger constant.

Note that in Example 1.2, as the size of the graphs increase the Cheeger constant decreases, and assuming that the Cheeger constant is a good measure of structural integrity, the structures become weaker.

### 2.1. *Other measures of structural robustness*

There are many purely graph theoretic measures other than the Cheeger constant that may be relevant to structural robustness. Perhaps the most obvious is the degree of each vertex in the graph. It is intuitively obvious that if the degrees of the vertices are higher, then there can be more interconnections between parts of the graph and so it can be a stronger structure. However, higher vertex degree is not sufficient on its own. For example, we can imagine constructing a graph with degree 3 at each vertex as follows: Take a tree with every internal vertex having degree 3, and then add a loop (an edge with both ends at the same vertex) to each leaf vertex. The result would have only a single edge linking any two subsets of the graph, and there would therefore be many potential weakpoints.

Another purely graph theoretical measure is the **girth** of a graph, defined to be the length of a shortest cycle in the graph. This seems relevant to “local rigidity”. In particular, structures involving triangles (i.e. having cycles of length three) are generally stronger than structures with only longer cycles. However, the girth would be three for both a graph with a single triangle and the rest of the structure quite sparsely connected, and for a dense structure with a large number of triangles. The former would not be very robust in comparison with the latter. The girth as defined is a “local” measure, because for any graph it can be reduced to three by simply adding a triangle to any part of it. In contrast, the Cheeger constant is more global, and cannot generally be increased significantly by altering only one arbitrarily chosen, small region of the graph.

There are also many features of the particular realisation of an abstract graph as a physical object in space of importance, such as the relative lengths and angles between edges. However, for the reasons given above, we feel that the Cheeger constant gives a reasonable “first approximation” for comparison between structures, at least when all edge lengths and angles are standardised, as in the case of graphs based on a regular lattice. In particular, one could represent a graph with a design involving intersections between edges other than at their endpoints. The extra intersections would help with structural stability, but since they are not represented in the graph the Cheeger constant would not take them into account (nor would any purely graph theoretical measure).

If one were to make a large scale physical sculpture of a graph, one would need to perform a proper computer analysis of structural integrity, and of course we do not claim that the Cheeger constant would replace such an analysis. However, investigating graphs that maximise the Cheeger constant under given constraints (e.g. a fixed vertex degree) may lead to interesting and novel structures that we would also expect to be robust.

### 3. Space filling curves and iterated substitution

The first space filling curve was discovered by Peano [8] in 1890, and a simpler construction was found by Hilbert [4] in 1891. See Figure 1 for three steps in the construction of the Hilbert curve. Note that the steps in this construction are not closed curves, although there is a closely related space filling curve (due to Moore) that does have closed curve steps. For the purposes of generalisation, we view these curves as graphs embedded in the plane, and we view the construction as follows:

We start with a base graph as in the leftmost diagram of Figure 1. To get the second graph, we substitute each vertex  $v$  with a **vertex replacement graph**  $G_v$  (in this case consisting of 4 vertices and 3 edges), and we substitute each edge  $e = (v_1, v_2)$ <sup>1</sup> with an edge  $e' = (v'_1, v'_2)$  (shown in Figure 1 as a dotted line), where  $v'_i \in G_{v_i}$  for  $i = 1, 2$ .

In this case there are choices to make in the orientation of the vertex replacement graphs  $G_v$  which ensure that the new edges are parallel to the grid lines, and that they do not cross over each other, or parts of the  $G_v$ . The space filling curve constructed by Hilbert is constructed as a limit of these steps, and there are many similar constructions. We will be more interested in the steps in the construction.

### 4. Fractal graphs by iterated substitution

We wish to generalise this construction to allow the degrees of vertices to be greater than 2. There are however some conditions that must be met, even at the level of the graph theory (i.e. ignoring for the moment the embedding into the plane). For example, suppose we want to make a construction again based on a square grid, but this time with degree 3 vertices. Let  $v$  be a vertex at some stage of the construction. If our vertex replacement graph  $G_v$  has 4 vertices again, then of the 12 ends of edges incident to the 4 vertices, 3 of them are “external”, connecting to some graphs  $G_{v'}, v' \neq v$ , leaving 9 which must be on edges internal to  $G_v$ . This is clearly impossible, since each edge contributes two ends. We will see the more general form of this condition in Theorem 4.3.

To solve this, we can either change the number of vertices in the vertex replacement graph, or we can change the number of edges in stage  $n + 1$  which replace an edge at stage  $n$ . See Figure 3 for an example in which we replace one edge with two at each stage.

Allowing this generalisation, we make the following definition:

**Definition 4.1** A sequence of **iterated substitution graphs**,  $F_1, F_2, \dots$  is generated by a **base graph**  $B = F_1$ , together with a set of substitution rules that produce  $F_{n+1}$  given  $F_n$ . The substitution rules have the following form: We have a set  $\mathcal{R} = \{R_1, R_2, \dots, R_k\}$  of **vertex replacement graphs**, together with a map  $r$  which takes a vertex  $v$  of  $F_n$  to an element of  $\mathcal{R}$ , and an integer  $M$  (the **edge replacement multiplicity**). We replace each vertex  $v$  with  $R_v \cong r(v)$ . We replace each edge  $e = (v_1, v_2)$  with a set  $E_e$  of edges  $e'$ , where  $|E_e| = M$  and for each  $e' = (v'_1, v'_2)$ ,  $v'_i \in R_{v_i}$  for  $i = 1, 2$ .

We will generally consider these graphs to be embedded in Euclidean space, and that the map  $r$  from the vertices of  $F_n$  to  $\mathcal{R}$  performs the function of recognising the local geometry of the edges incident to the vertex and choosing the correct replacement graph (and orientation). In the construction of the Hilbert curve for example, we have vertices with two edges either

---

<sup>1</sup>In this paper we view embeddings of graphs into Euclidean space as being given by the positions of the vertices, and edges connecting their endpoints linearly. We then view the data of an edge as just being the pair of vertices that are its endpoints.

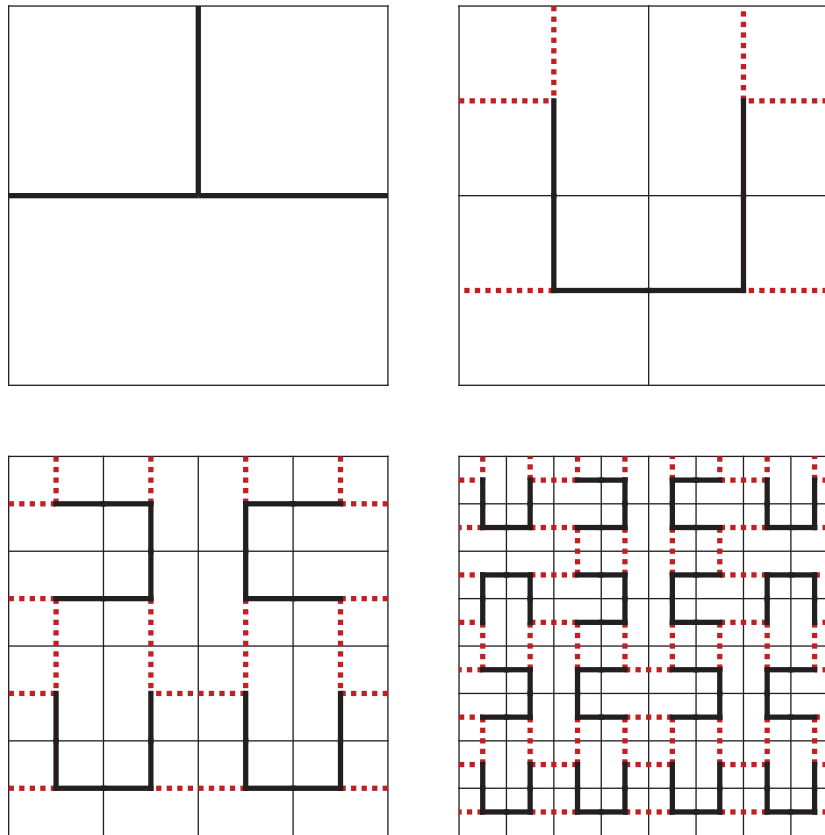


Figure 3. Four stages of part of an iterated substitution graph with edge replacement multiplicity 2. Each edge at stage  $n$  is replaced by two parallel edges in stage  $n + 1$ . Edges extend past the top, left and right boundaries of each diagram, in order that every vertex has degree 3 (which is a requirement for performing the substitution move to obtain the next stage). If we wanted to make a finite design based on this substitution rule, we would have to start with a finite degree 3 graph. There is no such finite degree 3 graph subset of the square lattice, although one could make such a construction on a torus, or the surface of a cube.

incident at 90 degrees, or at 180 degrees. It happens that the vertex replacement graphs for these two cases are the same up to orientation, but this will not be true in general.

With an embedding into Euclidean space we could also consider the limiting object as a subset of Euclidean space. Most of the examples in this paper have space filling limits, and so the corresponding limiting objects will be dense within the square or cube of space they occupy. In section 4.5 we will see some examples that are not space filling, and so the limiting object is more interesting.

#### 4.1. Iterated substitution graphs of fixed degree

From now on we will restrict to the case for which every vertex of each iterated substitution graph in the sequence has the same degree  $D$ , and we call this a sequence of **iterated substitution graphs of degree  $D$** . Note that the vertices of each vertex replacement graph  $R_i$  will have degrees less than or equal to  $D$ , and those vertices for which the degree is strictly less than  $D$  will have the deficit made up by edges from the  $E_e$ .

**Theorem 4.2:** *Let  $G$  be a vertex replacement graph for an iterated substitution graph of degree  $D$ , with edge replacement multiplicity  $M$ , vertex set  $V$  and edge set  $E$ . Then:*

$$D(|V| - M) = 2|E|$$

*Proof* This follows from counting the total number of ends of edges incident to vertices in  $V$  in two different ways, first by looking at the degrees of the vertices, and second by multiplying the number of edges by 2.  $\square$

For any curve,  $D = 2$  and  $M = 1$ , so this becomes  $|V| - 1 = |E|$ , which tells us the unremarkable fact that we must replace a vertex with a piecewise linear curve.

There is also a converse statement:

**Theorem 4.3:** *If  $D, M, N_V, N_E$  are positive integers such that  $D(N_V - M) = 2N_E$  then there exists a vertex replacement graph  $R$  for an iterated substitution graph of degree  $D$ , with edge replacement multiplicity  $M$ , vertex set  $V$  and edge set  $E$ , and  $|V| = N_V, |E| = N_E$ .*

*Proof* We can build the graph  $R$  by starting with  $N_V$  vertices and then arbitrarily adding edges between pairs of vertices that do not yet have  $D$  ends of edges incident. The two vertices need not be distinct and thus loops may occur. We stop only when we have added  $N_E$  edges, and then because  $D(N_V - M) = 2N_E$ , we have exactly the right deficit of degrees of vertices less than  $D$  to attach the  $MD$  edges that replace the  $D$  edges from the previous iterated substitution graph in the sequence.  $\square$

#### 4.2. Iterated substitution graphs on square lattices

So far we have considered only the topological properties of iterated substitution graphs. In this section we specialise to iterated substitution graphs for which each stage is a subset of a square lattice, and consecutive lattices are related by a scaling factor of 2. The edge replacement multiplicity can be either 1 or 2, and the degree can be 0,1,2,3 or 4. Degrees 0 and 4 are trivial, and degree 2 (i.e. fractal curves on square lattices) is already well studied, although it is an interesting exercise to investigate the cases for which  $|V| < 4$ . The case of degree 1 is surprisingly interesting: Theorem 4.3 becomes  $|V| - M = 2|E|$ , and so the number of vertices must have the same parity as the edge replacement multiplicity.

- If  $|V| = 1$  then  $M = 1, |E| = 0$ , and an edge is replaced at the next stage with another single edge (in one of two possible positions). As we generate further stages, initial edges of the pattern “shrink down”, and we get a very sparse pattern, with each stage having the same number of edges as the original pattern.
- If  $|V| = 2$  then  $M = 2, |E| = 0$ , and an edge is replaced in a unique way by two parallel edges in the next stage. As we continue, at the  $n$ th stage, each initial edge has become  $2^{n-1}$  parallel edges.
- If  $|V| = 3$  then  $M = 1, |E| = 1$ , and an initial edge is replaced by one edge joining two subsquares of the squares around the initial edge (in one of two possible places), with the internal edge of each replacement graph “bracketing” the edge replacement. The choice here means that there are many possibilities in later stages.
- If  $|V| = 4$  then  $M = 2, |E| = 1$ , and we have a unique way to construct each stage from the previous. See Figure 4. This construction replicates the Domino pattern (discovered by F. Lançon, see [http://tilings.math.uni-bielefeld.de/substitution\\_rules/domino](http://tilings.math.uni-bielefeld.de/substitution_rules/domino)).

In the case of degree 3, Theorem 4.3 becomes  $3(|V| - M) = 2|E|$ , and we must have  $|E| = 3$ . It isn't hard to check that the case of  $M = 1$  has no solutions on the square grid, and that the only solution is the one shown in Figure 3.

#### 4.3. Iterated substitution graphs on cubic lattices

There are many more possibilities when we move to three dimensions, so we will only mention a few interesting constructions, chosen either for aesthetic reasons or for simplicity of their

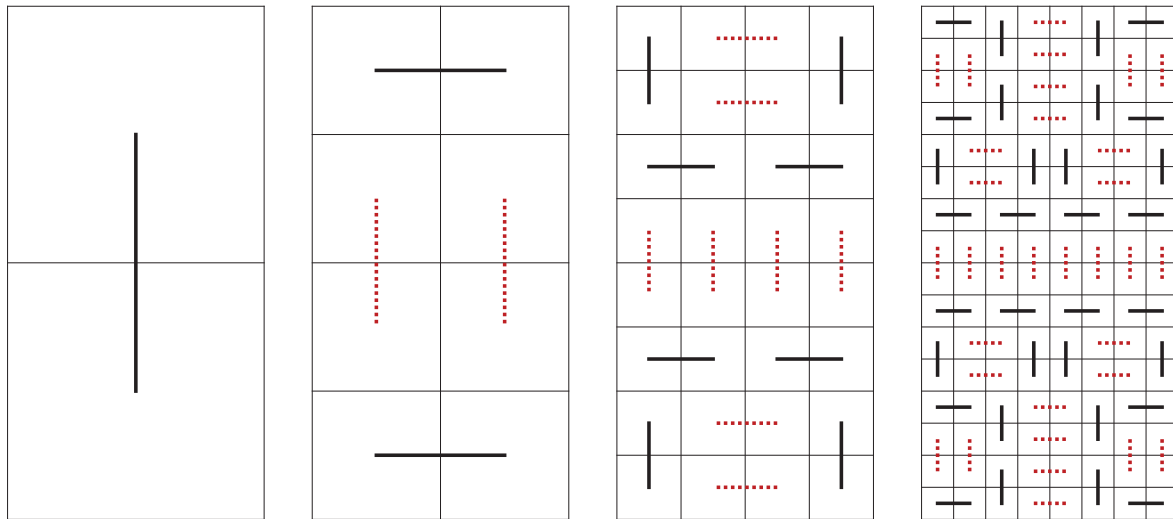


Figure 4. Four stages of an iterated substitution graph with degree 1 and edge substitution multiplicity 2. Each edge at stage  $n$  is replaced by two parallel edges in stage  $n + 1$ .

description.

First suppose that we want to use cubic lattices with the scaling factor between consecutive lattices being 2, and that we want the limiting object to be space filling, meaning that we must have  $|V| = 8$ . If we also want  $M = 1$ , then we run into trouble for  $D > 2$ : Theorem 4.3 becomes  $7D = 2|E|$ . For  $D = 3$  the left hand side is odd, and for  $D \geq 4$  we get that  $|E| \geq 14$ , but there are only 12 possible edges to use for the cubical vertex replacement graph.

There are a number of interesting ways to work around this “first try” at generalising the steps in the construction of a 3-dimensional space filling curve to a sequence of graphs. First, we can alter the scaling factor between consecutive lattices from 2 to 3, and then we do have a solution for  $M = 1, D = 3$ . Note that for  $D = 3$  and a graph on a cubic lattice, there are two possible configurations of edges incident to a vertex: Either the three edges are mutually perpendicular (we call this configuration a **tripod**), or two edges are in opposite directions and the third is parallel to the first two (we call this configuration a **T**). Then we can use vertex replacement graphs as shown in Figure 5.

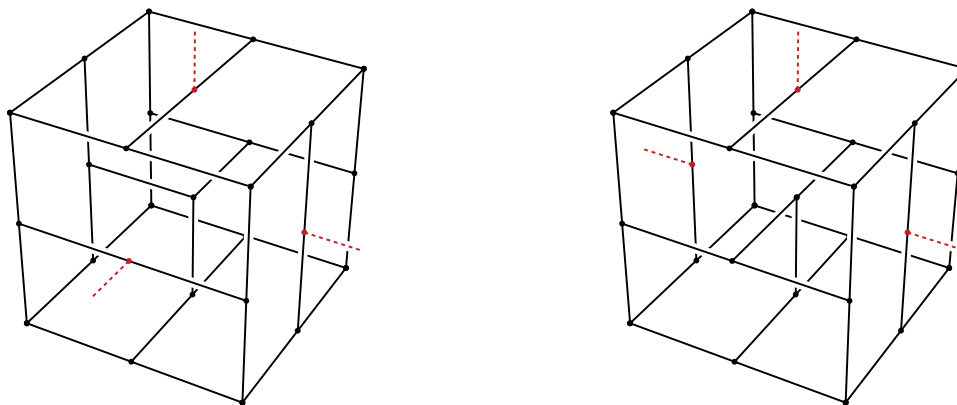


Figure 5. Vertex replacement graphs for a tripod (on the left) and a T (on the right), for a cubic lattice iterated substitution graph in which  $D = 3, |V| = 27, M = 1$  and so  $|E| = 13$ .

If we fix as a requirement that the vertices of the vertex replacement graphs at which the

replacements for the edges connect are in the centers of three faces, then these solutions are unique up to orientation. Figure 6 shows the result of starting with the 1-skeleton of a cube and substituting twice, with these choices of orientation.

One disadvantage of this solution from the viewpoint of physical construction is that the 8 octants of the graph are connected to each other only by edges corresponding to the edges of the base graph, which is a cube. Thus a good guess for the subset of the graphs in Figure 6 that gives the minimum in the expression for the Cheeger constant would be to take an orthogonal half. Such a half is connected to the other half by only 4 edges. In fact this guess is correct, by the following result:

**Theorem 4.4:** *Suppose that a sequence  $\{F_n\}$  of iterated substitution graphs with edge replacement multiplicity 1 and degree  $D$  has vertex replacement graphs  $R_i$ , all of which have the same number  $N_V$  of vertices, and with the property that for any non-empty set of vertices  $C \subset R_i$ ,  $|\partial C| \geq D$  (here if  $C$  includes any vertices of degree less than  $D$  we add the degree deficit to  $|\partial C|$ ). Moreover suppose that the number of vertices in  $F_1$  is even. Then the Cheeger constant for  $F_n$  is achieved by taking a subset  $A_0$  of the base graph  $F_1$  that achieves its Cheeger constant, then building the subset of  $F_n$  from the descendants (via the vertex replacement graphs) of the vertices in  $A_0$ .*

We postpone the proof to the appendix. This result allows us to directly calculate the Cheeger constant for many iterated substitution graphs when the edge replacement multiplicity is 1. However, their Cheeger constants will all be quite small, as the minimum is achieved by splitting the graph at the same number of edges as are required in the minimum for the base graph. As we will see in section 4.4, we can do better when we allow edge replacement multiplicities greater than 1, the cases for which Theorem 4.4 does not apply.

In the present case, it is easy to convince oneself that no subset of the graphs in Figure 5 with at least one vertex can have a boundary of size strictly smaller than 3 (this could also be checked by exhaustive search). Moreover, the edge replacement multiplicity is 1, so the theorem holds.  $F_1$  is a cube, and for this graph the Cheeger constant is achieved with  $A_0$  being the four vertices making up a square face. Thus, for this case,  $F_n$  has  $|V| = 8 \times 27^{n-1}$ , and  $h(F_n) = \frac{4}{4 \times 27^{n-1}} = 27^{1-n}$ .

In contrast, we can look at the “full cubic lattice” graphs  $C_N$ , defined as follows:  $C_N$  has vertices  $\{1, 2, \dots, N\}^3 \subset \mathbb{Z}^3$  and has edges between every pair of vertices that are distance 1 apart.

**Proposition 4.5** If  $N$  is even then  $h(C_N) = \frac{2}{N}$ .

Again, one might guess that taking an orthogonal half subset would give the minimum in the expression for the Cheeger constant, and again this is correct. We defer the proof of the proposition to the appendix.

**Remark 4.6** The graph  $C_N$  will have the highest possible Cheeger constant of any graph that has the same vertices but a subset of the edges. This is true because for any candidate subset  $A$ ,  $|\partial A|$  can only be larger for  $C_N$  when compared to some other graph.

This observation implies that since  $h(C_N)$  decreases with  $N$ , the Cheeger constants for any of these subsets of cubic lattices will also go down as the size increases. However, we are interested in how quickly or slowly it decreases. We have seen that  $h(C_N) = \frac{2}{N} = 2|V|^{-\frac{1}{3}}$ . In comparison, the graphs generated by the rules in Figure 5 have  $h(F_n) = 27^{1-n} = 8|V|^{-1}$ , and a closed curve has  $h(G) = \frac{2}{|V|^{1/2}} = 4|V|^{-1}$ . See Figure 7 for a graphical comparison of these examples, and other examples from later in the paper.

The results of this section show that if the edge replacement multiplicity  $M = 1$  and the vertex

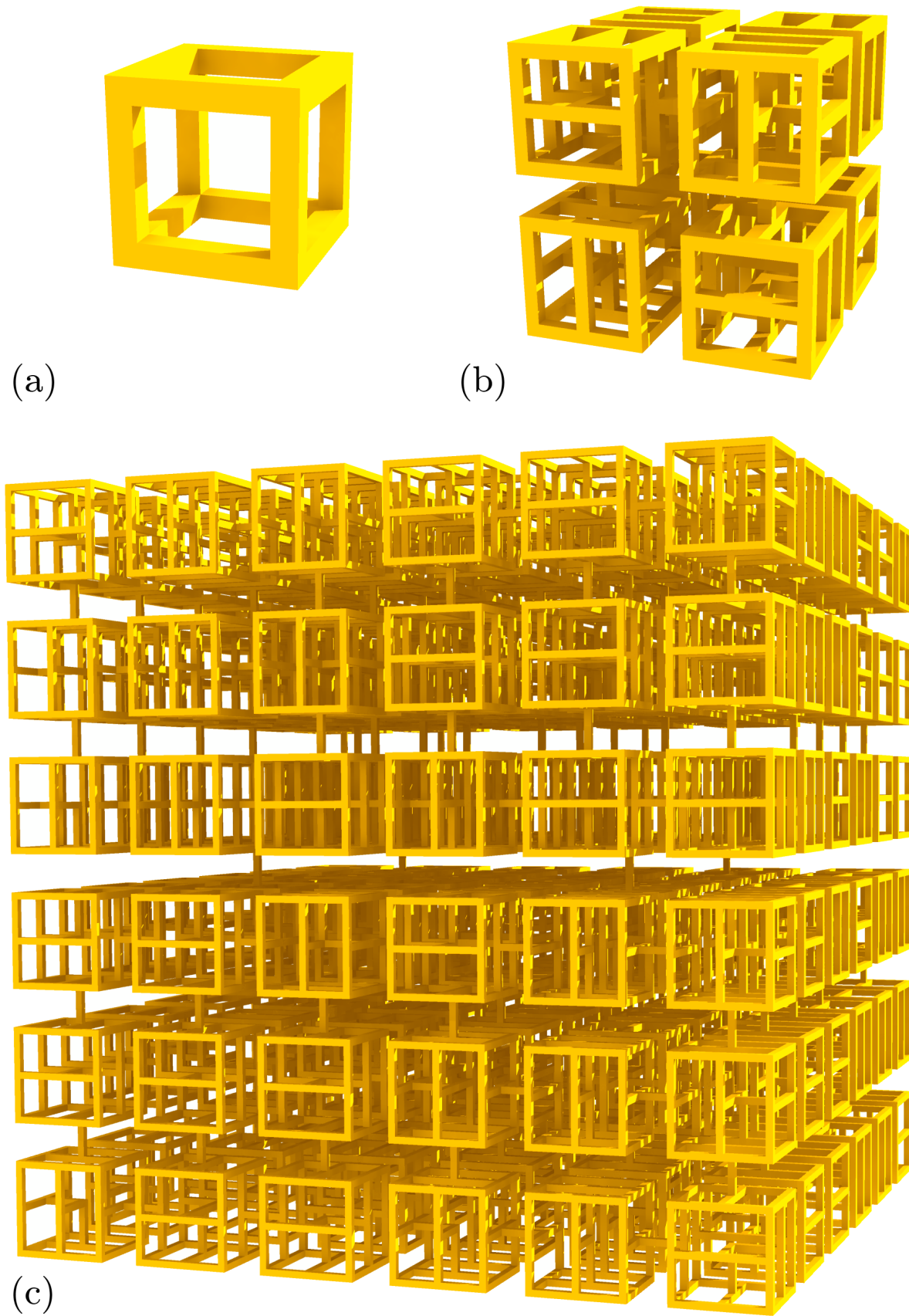


Figure 6. Three stages of an iterated substitution graph for which  $D = 3$ ,  $|V| = 27$  and  $M = 1$ .

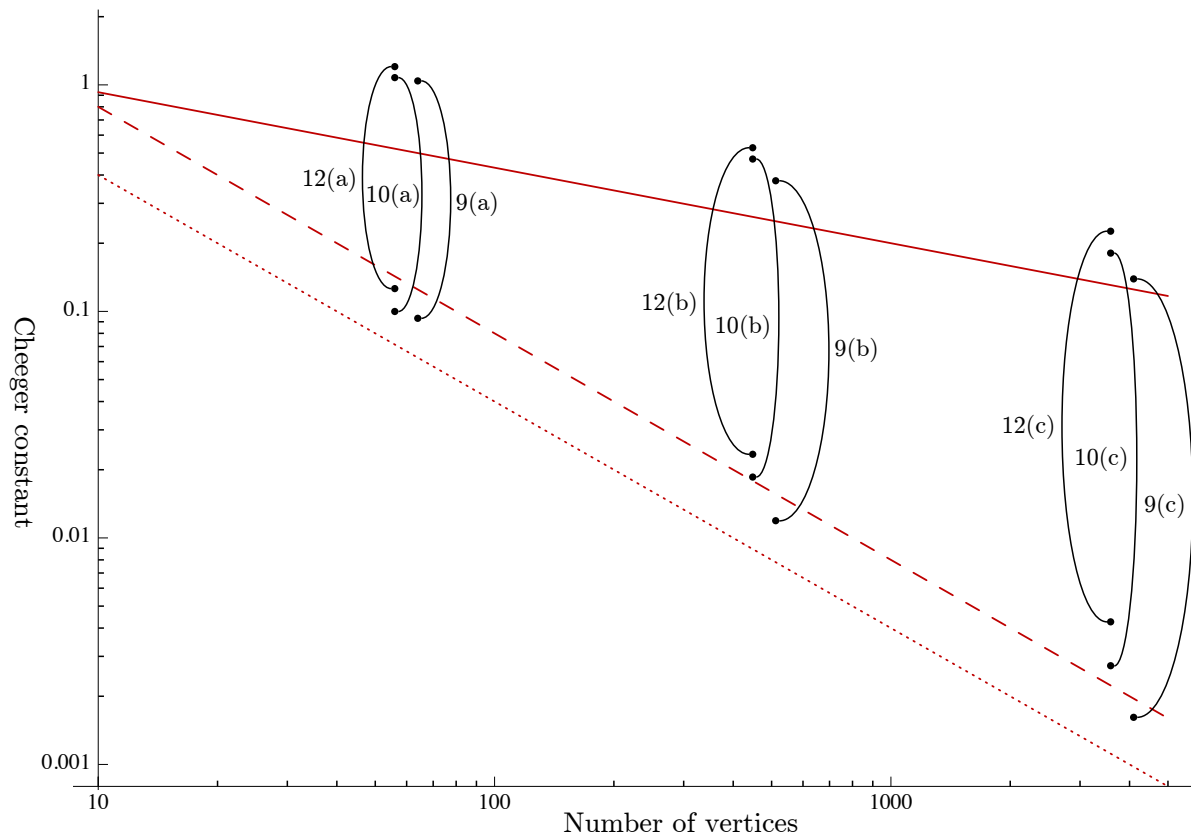


Figure 7. Log-log plot of number of vertices against the Cheeger constant. The solid line is the plot for a cubic subset of the cubic lattice,  $C_N$ . The dotted line is the plot for a closed curve. The dashed line is the plot for the examples of Figure 6. The brackets are bounds as in Theorem 4.7 for the graphs in Figures 9, 10 and 12.

replacement graphs themselves are not too “bottlenecked”, then we won’t do much better than closed curves in terms of larger Cheeger constants. Thus, we move to higher edge replacement multiplicities.

#### 4.4. Edge replacement multiplicity greater than 1

In this section we exhibit some examples of iterated substitution graphs on cubic lattices, with edge replacement multiplicity greater than 1. We would like to compare their Cheeger constants with those of the graphs from the previous section. Unfortunately, we do not have a way to efficiently calculate the exact values of their Cheeger constants, and calculating Cheeger constants of graphs precisely is a difficult problem in general. However, we can calculate bounds using Cheeger’s Inequality, given in the following theorem. We use a formulation due to Mohar [5], although the ideas appear in many papers, one of the earliest being by Alon and Milman [1]. Terms used in the theorem are described after the statement.

**Theorem 4.7** (Theorems 4.1 and 4.2 of [5]) *Let  $L$  be the Laplacian matrix of a finite graph  $G$ . All eigenvalues of  $L$  are real and non-negative. Let  $\lambda_1$  be the second smallest eigenvalue of  $L$ . Then:*

$$\frac{\lambda_1}{2} \leq h(G)$$

*and moreover, if  $\Delta$  is the maximal vertex degree and  $G$  is not equal to any of  $K_1, K_2$  or  $K_3$  then:*

$$h(G) \leq \sqrt{\lambda_1(2\Delta - \lambda_1)}$$

The Laplacian matrix of a finite graph  $G$  is an  $n \times n$  square matrix where  $n$  is the number of vertices in  $G$ . Each row and column corresponds to a vertex of  $G$ . It is calculated as  $L = D - A$ , where  $A$  and  $D$  are given as follows. Let  $A$  be the adjacency matrix of  $G$ . That is,  $A$  has a “1” entry at row  $i$  and column  $j$  if and only if the vertices corresponding to  $i$  and  $j$  have an edge between them. All other entries are zero.  $D$  is a diagonal matrix with entries being the degrees of the corresponding vertex of the graph. The graphs  $K_1, K_2$  and  $K_3$  are the complete graphs on 1, 2 and 3 vertices respectively. A graph is complete if every vertex is connected to every other vertex by an edge, and so  $K_1$  is just a single point,  $K_2$  has two vertices and the edge between them, and  $K_3$  is a triangle.

We use the python package NetworkX [3] to calculate the eigenvalues of the graphs we exhibit in this section, and list the results in Table 1.

4.4.1. *The edge swap move*

We introduce a useful trick for constructing some kinds of iterated substitution graphs, the **edge swap move**. See Figure 8.

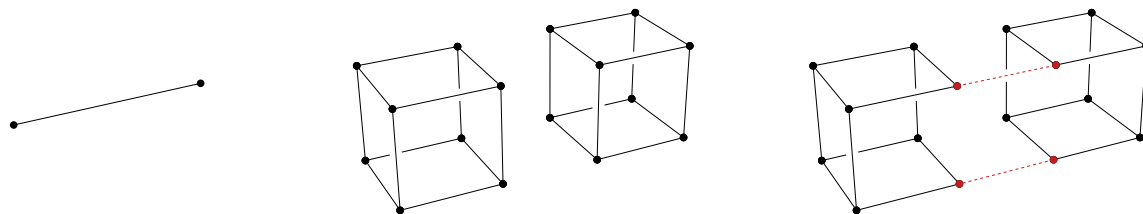


Figure 8. The edge swap move: We replace each vertex by a cube, then swap two edges in two neighbouring cubes with two edges which connect those two cubes together. For edge replacement multiplicity 2 and degree 3, this move generates a set of vertex replacement graphs.

If we start with a degree 3 graph  $G$  on a cubic lattice, replace each vertex by a cube and then perform edge swap moves for each edge of  $G$ , then we generate the next iterated substitution graph with edge replacement multiplicity 2. By construction all vertices in the result will have degree 3. In order to be able to perform this move for all of the edges of  $G$ , we need to make sure that we do not try to remove the same edge from some cube more than once. This can be achieved as follows:

We fix a cyclic ordering  $\sigma$  on the directions of the axes, say x-axis  $\xrightarrow{\sigma}$  y-axis  $\xrightarrow{\sigma}$  z-axis  $\xrightarrow{\sigma}$  x-axis). If  $G$  has an edge in the direction of an axis  $A$ , then we perform edge swap moves so that two edges of neighbouring cubes in the direction of axis  $\sigma(A)$  are replaced by two edges between those cubes in the direction of axis  $A$ . This ensures that there are no collisions between the edges to be swapped.

Note that for each edge of  $G$  there is also a choice between which pair of edges to swap, the two pairs differing in the direction of the axis  $\sigma^2(A)$ . If we stick to a consistent choice of which pair to choose, we get Figure 9, which shows three stages of an iterated substitution graph using these rules.

4.4.2. *Further examples*

Instead of choosing one or the other possible pair of edges to swap, we can swap both pairs to give an iterated substitution with edge replacement multiplicity 4, as in Figure 10, starting with a cube. At the first stage after the cube, the graph has two components: a central cube and a more interesting outer component. From the point of view of a physical construction this is a

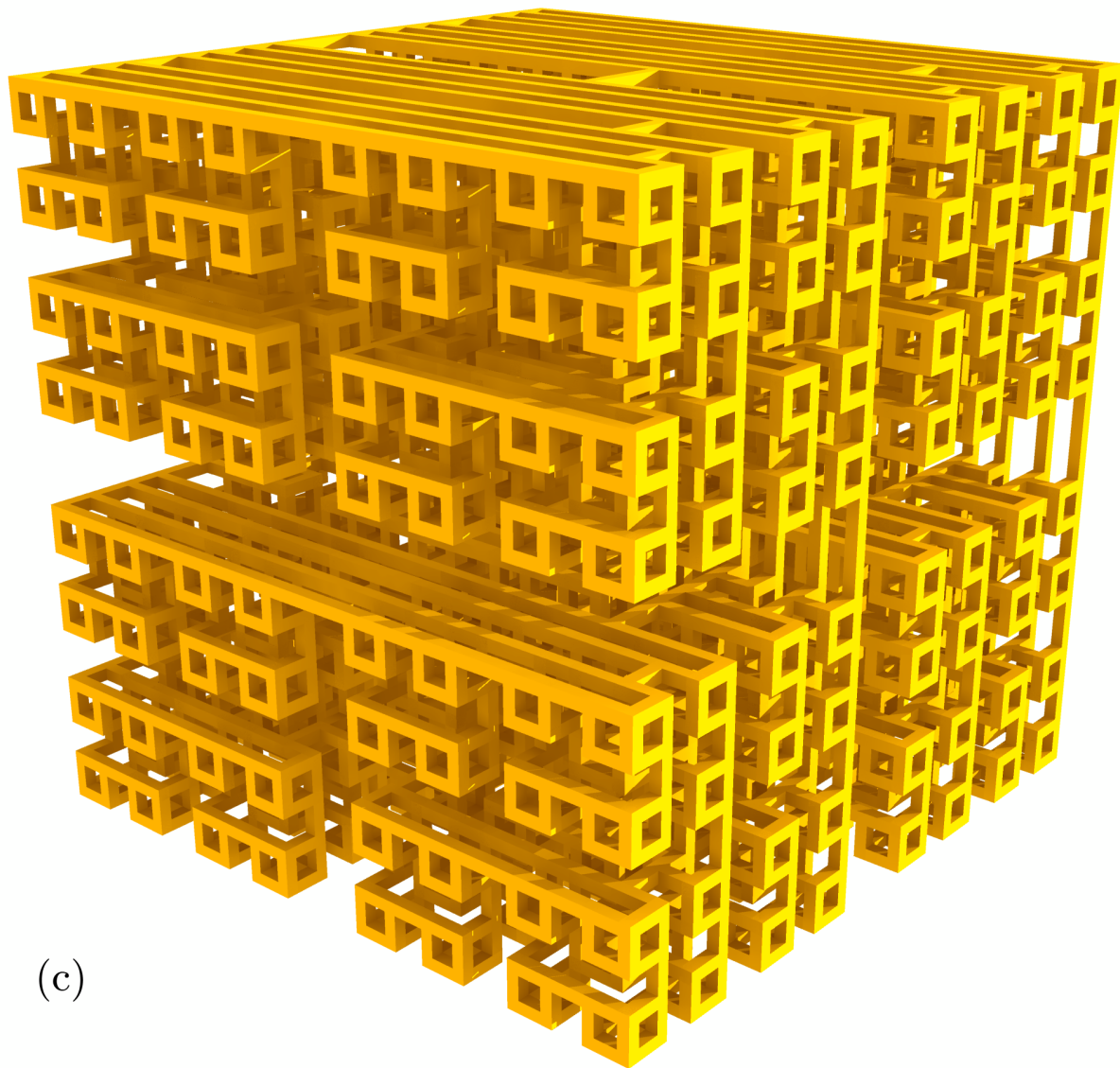
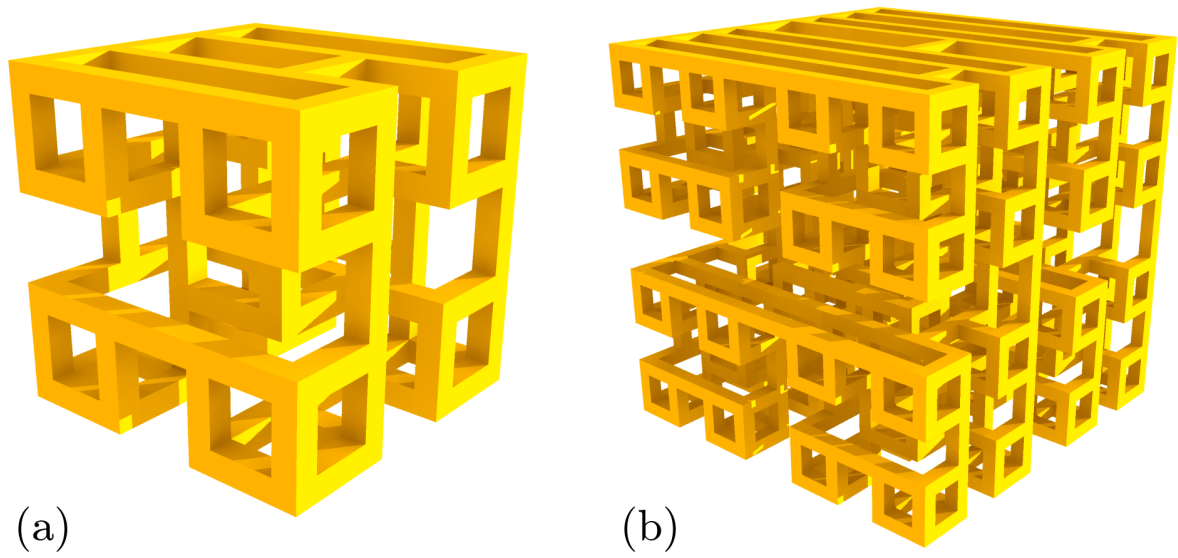


Figure 9. Three stages of an iterated substitution graph with degree 3 and edge replacement multiplicity 2. We start with a cube and use the edge swap move, choosing the pair of edges to swap in a consistent direction. To highlight the fractal structure, we have drawn this graph with varying spacing between the vertices.

problem, and also the Cheeger constant of any graph with multiple components is zero. To fix this, we discard the central cube at this stage. Further stages derived from this are connected. From an aesthetic point of view, the resulting empty space in the center can be seen as a desirable feature in that the detail of the outer structure is not lost in a confusing background formed by interior structure.

There are many other possibilities with edge replacement multiplicity 4. We give one further example, using the rules in Figure 11 to produce Figure 12. For replacements of T type vertices, we have chosen to orient the result so that the single edge component of the vertex replacement graph is closest to the center of the graph (as embedded in  $\mathbb{R}^3$ ). Again, we remove a central cube at the first stage after the cube. Figure 13 shows the result of 3d printing the third graph in Figure 12.

In Table 1 we list the upper and lower bounds for the Cheeger constants of the graphs in this section given by Theorem 4.7. Note that the (maximal) vertex degree in all of these graphs is 3.

Table 1. Cheeger bounds for the graphs in Figures 9, 10 and 12.

Graph	Number of vertices	$\lambda_1/2$	$\sqrt{\lambda_1(2 \cdot 3 - \lambda_1)}$
Figure 9(a)	64	0.09322	1.04107
Figure 9(b)	512	0.01191	0.37734
Figure 9(c)	4096	0.00161	0.13915
Figure 10(a)	56	0.09992	1.07659
Figure 10(b)	448	0.01856	0.47051
Figure 10(c)	3584	0.00272	0.18084
Figure 12(a)	56	0.12608	1.20390
Figure 12(b)	448	0.02340	0.52783
Figure 12(c)	3548	0.00426	0.22597

These bounds are also shown graphically in Figure 7. Note that the upper bounds we calculate here are not as good as the upper bound given by the Cheeger constant for the full cubic lattice graphs in Remark 4.6. However, we do see that the examples of Figures 10(b,c) and 12(b,c) (and (c) in particular) do have lower bounds better than that for the examples of Figure 6. Thus, assuming that our Cheeger constant measure of the physical strength of a sculpture representing a graph is valid, we have shown that these examples should be more robust as structures than the examples in previous sections of this paper, and certainly more robust than steps in the constructions of space filling curves.

#### 4.5. Non space filling examples

In this paper we have mostly looked at space filling examples, although there are examples of non space filling, fractal curves that can also be seen as iterated substitution graphs. In this section we exhibit two examples of sequences of interesting iterated substitution graphs (in 3 dimensions, and of degree greater than 2) that are not space filling.

##### 4.5.1. An example on the cubic lattice

See Figure 14 for the substitution rule. All vertices are degree 3 and are tripods (there are no T vertices), and the scaling factor is 3 between stages. Only 7 of the 27 possible vertices are used. Figure 15 shows the second, third and fourth stage, starting from the cube. Figure 16 shows a 3d printed realisation of the fourth stage. Unlike the 3d printed sculpture shown in Figure 13 this structure is quite flexible. It readily bends at the 4 edges linking one half of the sculpture to the other, as would be predicted by the Cheeger constant.

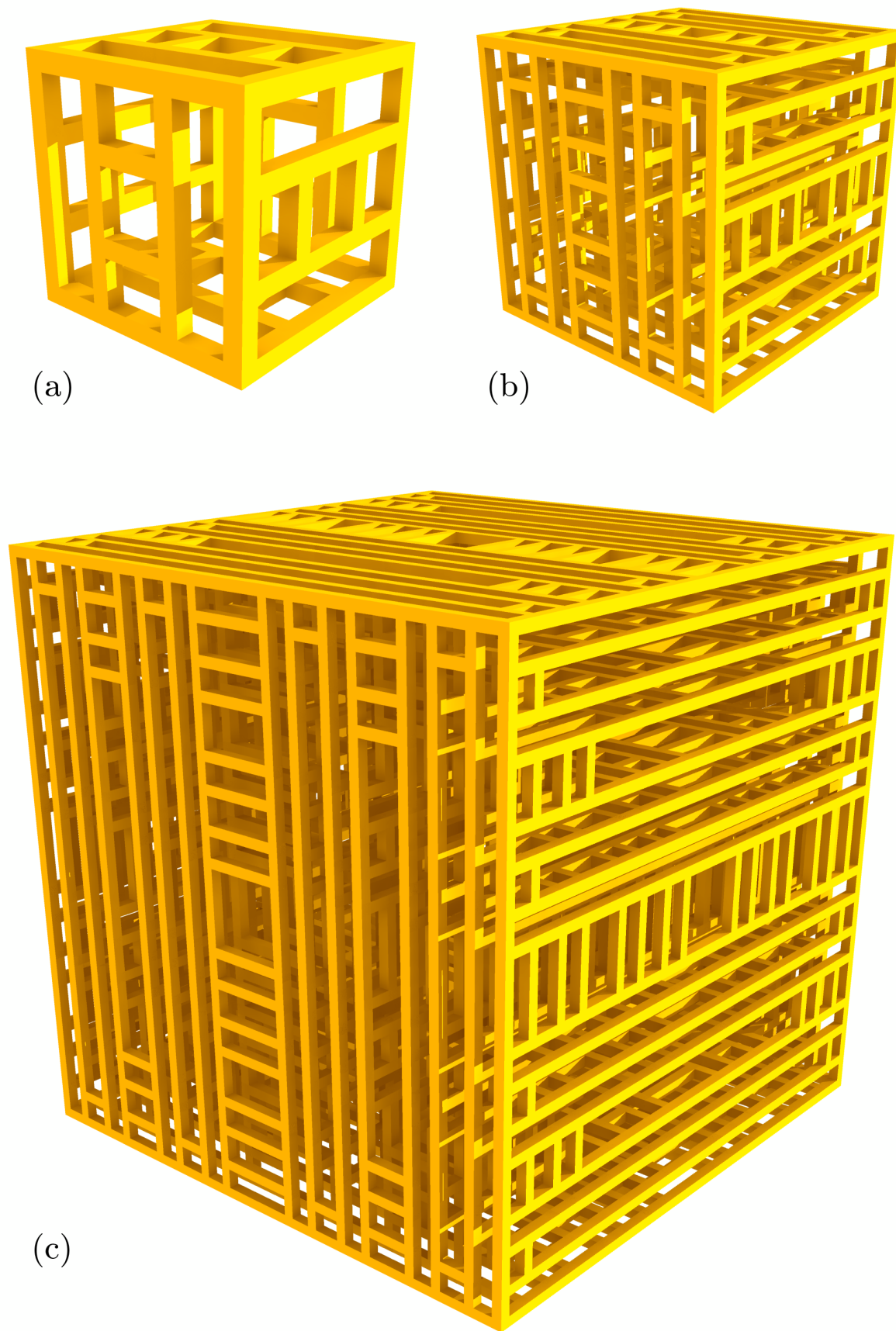


Figure 10. Three stages of an iterated substitution graph with degree 3 and edge replacement multiplicity 4. We start with a cube and use the edge swap move on both pairs of edges at each step. As before, to highlight the fractal structure we have drawn this graph with varying spacing between the vertices.

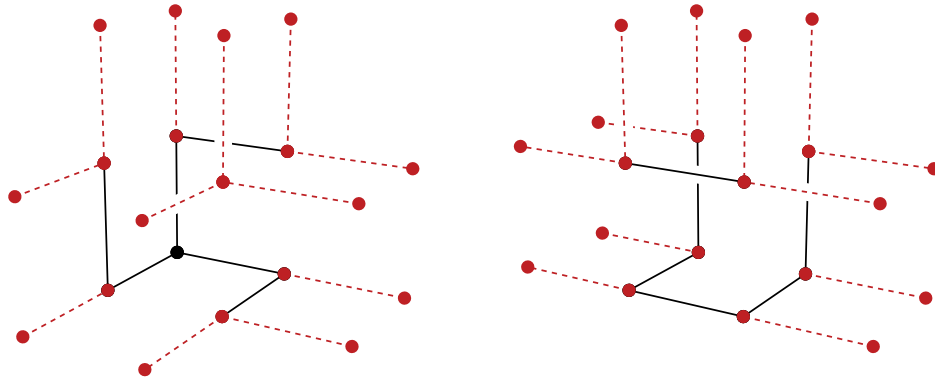


Figure 11. Vertex replacement graphs for iterated substitution graphs with degree 3 and edge replacement multiplicity 4. We replace a tripod with the graph on the left and a T with the graph on the right. There is a choice of orientation for the replacement of a T type vertex, and for Figure 12 we choose to orient so that the single edge component of the vertex replacement graph is closest to the center of the graph.

For this example, note that the limiting fractal starting from a tripod is self-similar, in the sense that if we take 7 copies of the fractal, each scaled down by a factor of 3, then we can arrange them to reconstruct the fractal. This implies that the Hausdorff dimension of the set is  $\frac{\ln(7)}{\ln(3)} \approx 1.7712$ . The Hausdorff dimension of all of the space filling graphs in this paper is either 2 or 3, depending on the dimension of the space that they fill.

#### 4.5.2. Octahedral lattice

Let  $E = \{(\pm 1, 0, 0), (0, \pm 1, 0), (0, 0, \pm 1)\}$ . Let  $E_0 = E$ ,  $E_1 = E_0 + 2^{-1}E$ , and more generally  $E_k = \sum_{i=0}^k 2^{-i}E$ . Then  $E_k$  gives the vertices of an “octahedral lattice”. The edges of the lattice are between all pairs of vertices at a distance of  $\sqrt{2}(2^{-k})$ . See Figure 17. This lattice itself does not fill space. (There are tetrahedron shaped gaps: we can think of each stage as being a subset of the octahedron/tetrahedron tessellation of space, and any points within tetrahedra at any stage will not be limit points of the sequence of lattices.)

Here we can use a trick very similar to the edge swap move to give rules to generate an iterated substitution graph of degree 4 and edge replacement multiplicity 2. See Figure 18. Unlike the edge swap move for the cubic lattice, there is no choice of which edges to swap.

Similarly to the cases of the examples in Figures 10 and 12, if we start with an octahedron then the second iterated substitution graph is not connected. There is an outer component around a central octahedron component. We again delete the central component and continue. See Figure 19 for the second, third and fourth stages. Figure 20 shows a 3d printed realisation of the fourth stage.

## 5. Conclusions

We have introduced a generalisation of the construction of space filling curves to a construction of space filling graphs, for which the steps retain the self similar structure but have greater connectivity. We have argued for the Cheeger constant as a reasonable measure of the structural strength we would expect in a physical representation of a graph (for example as a sculpture). We explored many of the possibilities for such graphs based on the 2 dimensional square lattice, and exhibited a few examples based on the 3 dimensional cubic lattice, which we were able to

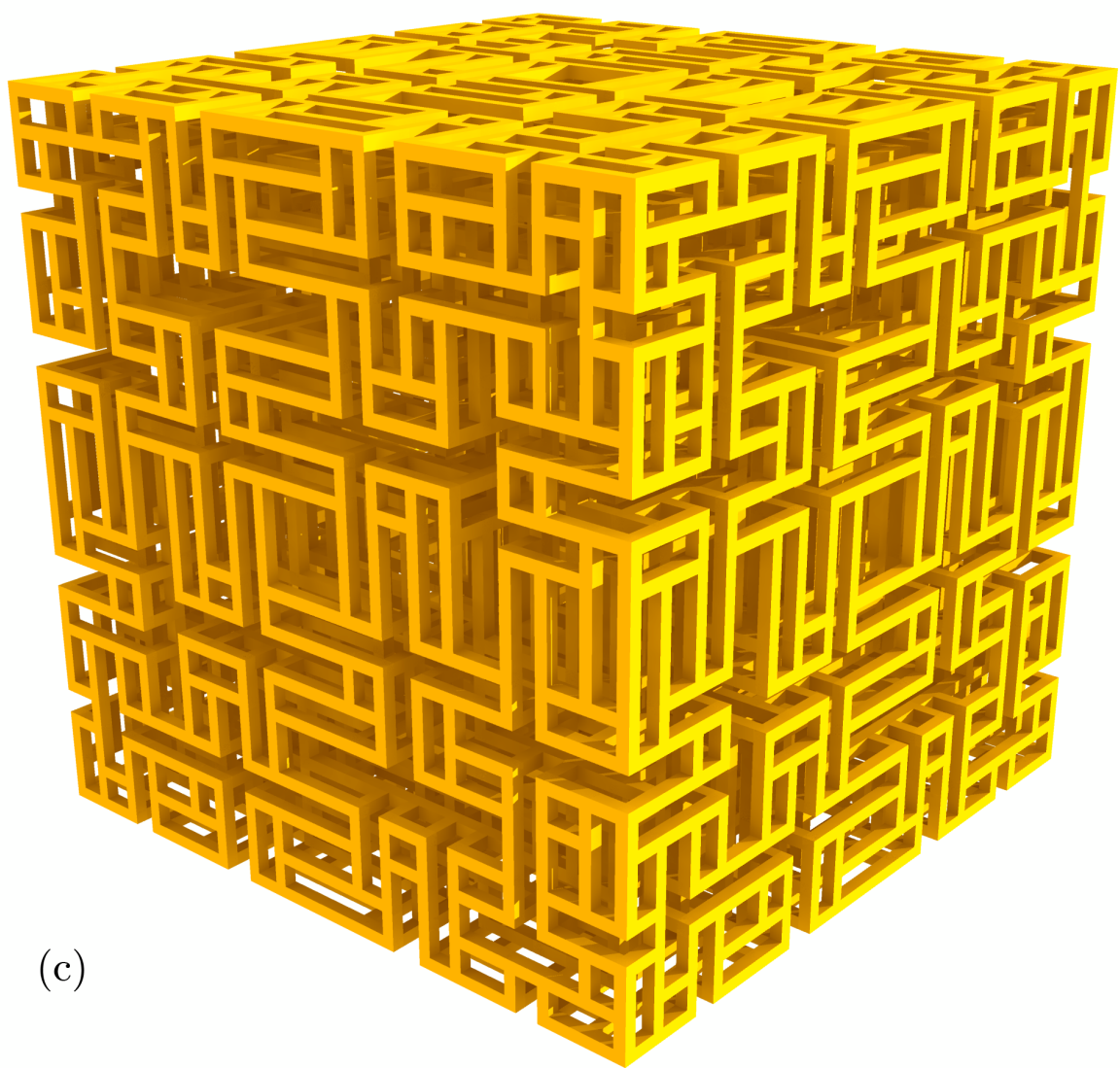
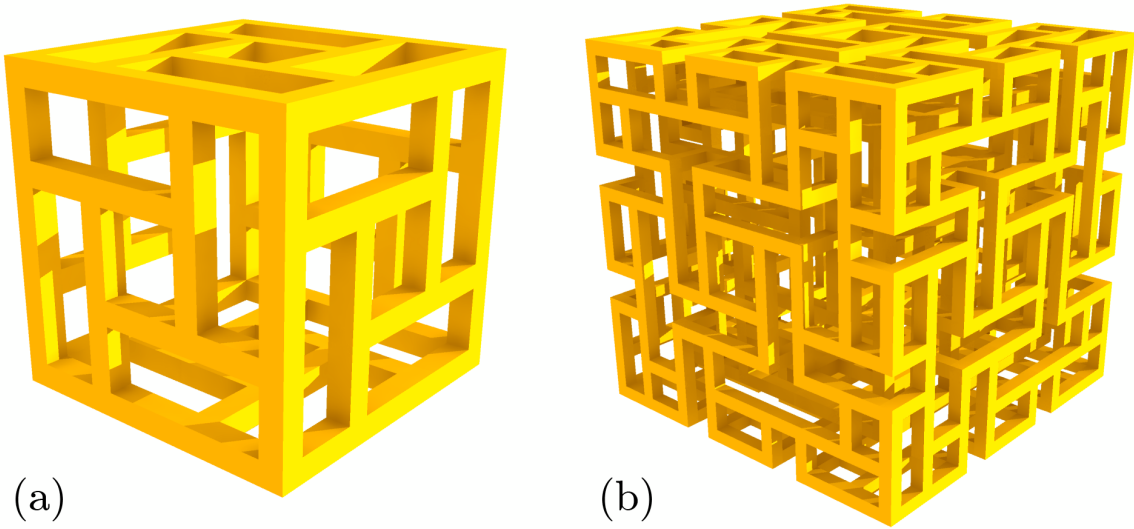


Figure 12. Three stages of an iterated substitution graph with degree 3 and edge replacement multiplicity 4, using the vertex replacement graphs as in Figure 11. As before, to highlight the fractal structure we have drawn this graph with varying spacing between the vertices.

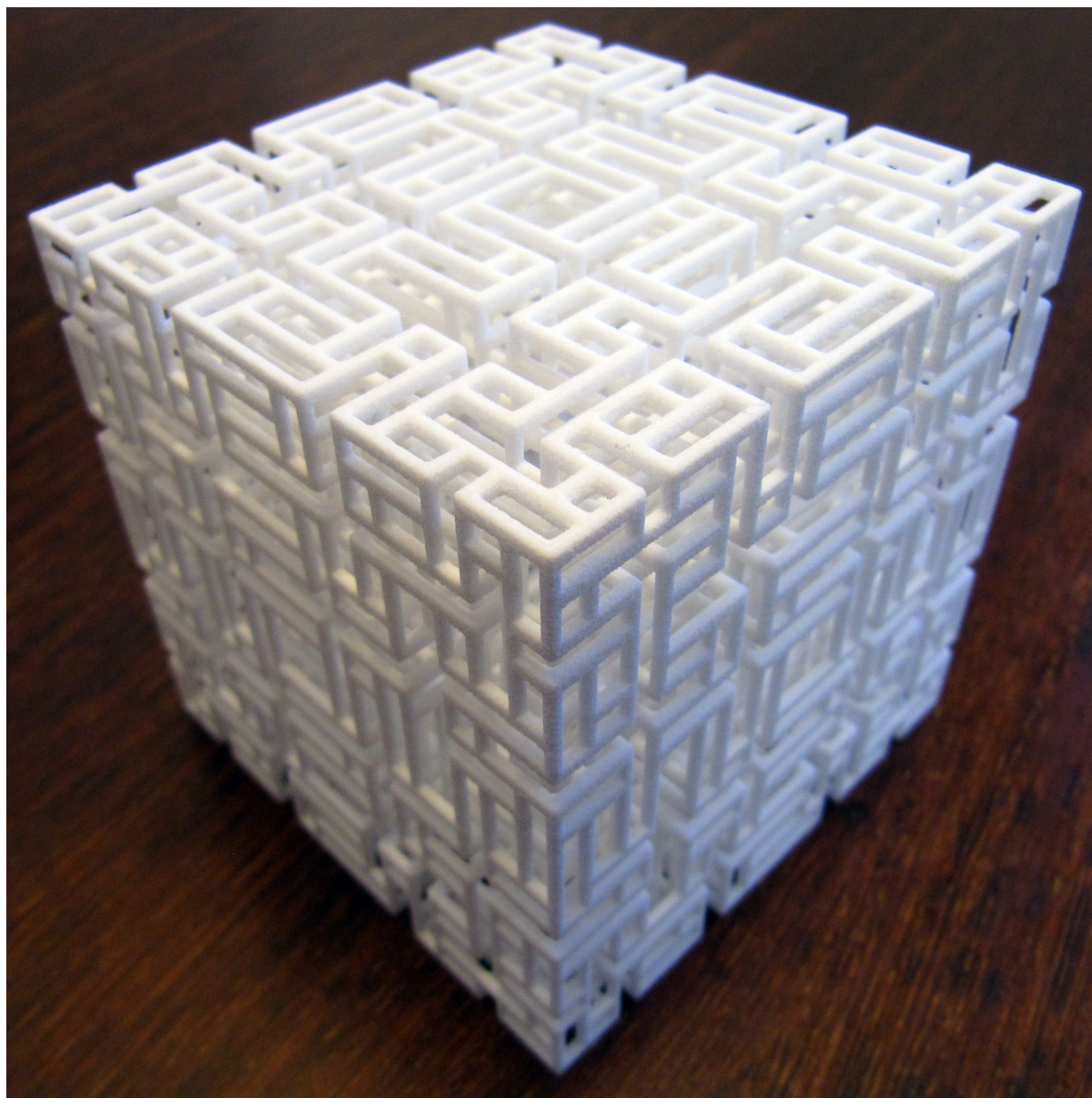


Figure 13. A 3d printed realisation of the third graph in Figure 12. The physical object is rigid.

compare to steps in the constructions of space filling curves and each other using the Cheeger constant measure. We believe that sculptures based on those designs with highest Cheeger constant should be considerably more robust than those with lower constants. Finally we gave two examples of aesthetically interesting iterated substitution graphs that do not have space filling limits.

A direction for future work would be to try to find iterated substitution graphs on the cubic lattice with degree 3 that have maximal Cheeger constant (for a given number of vertices). More generally one could drop the condition that the graph be constructed by iterated substitution, requiring only that the graph is a subset of the cubic lattice with degree 3, and ask which graph gives the maximal Cheeger constant. From a more aesthetic point of view, it seems that there are many more possibilities to explore within iterated substitution graphs, in particular when we drop the space filling condition or leave the cubic lattice.

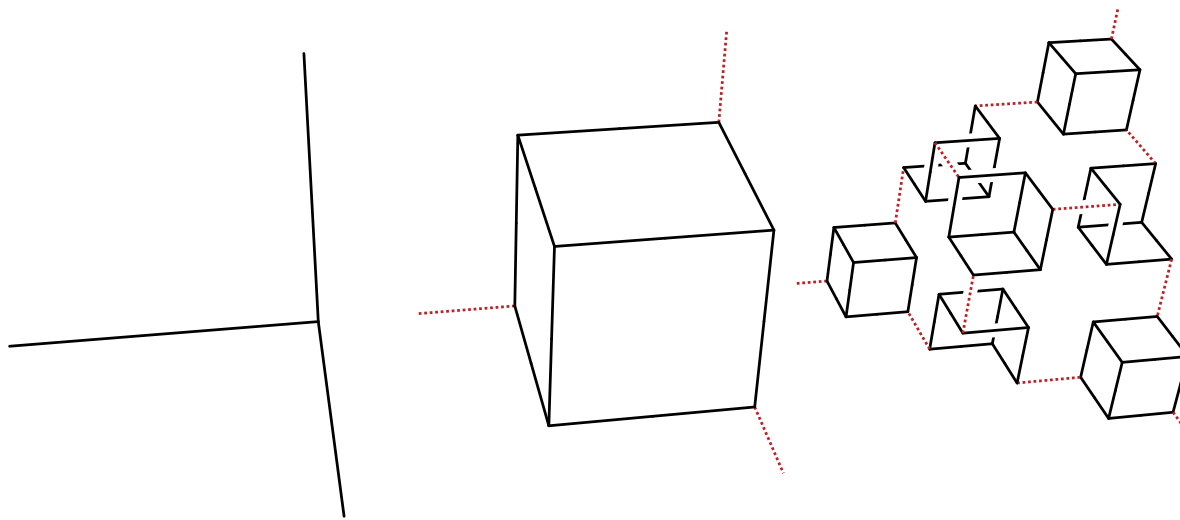


Figure 14. Three stages of part of an iterated substitution graph. Here  $D = 3$ ,  $|V| = 7$ ,  $M = 1$  and so  $|E| = 9$ .

## Acknowledgements

The author would like to thank Yla Tausczik for assistance in writing python programs to generate the graphs in section 4.4, and the referees for many helpful suggestions. The 3d printed sculptures were produced by Shapeways.com.

## References

- [1] N. Alon and V. D. Milman,  $\lambda_1$ , *isoperimetric inequalities for graphs, and superconcentrators*, Journal of Combinatorial Theory, Series B **38** (1985), 73–88.
- [2] Béla Bollobás and Imre Leader, *Edge-isoperimetric inequalities in the grid*, Combinatorica **11** (4) (1991) 299–314
- [3] Aric A. Hagberg, Daniel A. Schult and Pieter J. Swart, *Exploring network structure, dynamics, and function using NetworkX*, in Proceedings of the 7th Python in Science Conference (SciPy2008), Gael Varoquaux, Travis Vaught, and Jarrod Millman (Eds), (Pasadena, CA USA), pp. 11–15, Aug 2008
- [4] David Hilbert, *Ueber die stetige Abbildung einer Linie auf ein Flächenstück*, Mathematische Annalen **38** (1891), no. 3, 459–460.
- [5] Bojan Mohar, *Isoperimetric numbers of graphs*, Journal of Combinatorial Theory, Series B **47** (1989), 274–291.
- [6] Alexander Lubotzky, *Discrete Groups, Expanding Graphs and Invariant Measures*, Progress in mathematics (Boston, Mass.), Birkhäuser, vol. 125, 1994.
- [7] Vivien Muller, *Octocube*, <http://www.behance.net/Gallery/OctoCube/115645>, August 2008.
- [8] Giuseppe Peano, *Sur une courbe, qui remplit toute une aire plane*, Mathematische Annalen **36** (1890), no. 1, 157–160.
- [9] Carlo H. Séquin, *Hilbert Cube 512*, [http://www.cs.berkeley.edu/~sequin/SCULPTS/CHS\\_bronzes/Hilbert512/](http://www.cs.berkeley.edu/~sequin/SCULPTS/CHS_bronzes/Hilbert512/), Fabricated by Ex One Company, Prometal division, July 2005.

## Appendix A. Proofs

**Lemma A.1:** *Suppose that an iterated substitution graph  $F_n$  has the same properties as listed in Theorem 4.4. Then the minimum value of  $\frac{|\partial A|}{|A|}$  is achieved with a set  $A$  for which  $A \cap R_{v_i}$  is either  $\emptyset$  or  $R_{v_i}$ , for each  $v_i$  in the vertex set of  $F_{n-1}$ .*

Note that the edge replacement multiplicity being 1 is crucial to the following proof, and it seems very unlikely that a similar argument could be made to work for larger edge replacement multiplicities.

*Proof* Suppose we have a set  $A$  of the vertices of  $F_n$  such that  $0 < |A| \leq \frac{|V|}{2}$  and for some  $v_i$ ,  $A \cap R_{v_i}$  is neither  $\emptyset$  nor  $R_{v_i}$ . The plan is to alter  $A$  to  $A'$ , so that  $\frac{|\partial A'|}{|A'|} \leq \frac{|\partial A|}{|A|}$  and for all  $v_i$ ,  $A' \cap R_{v_i}$  is either  $\emptyset$  or  $R_{v_i}$ .

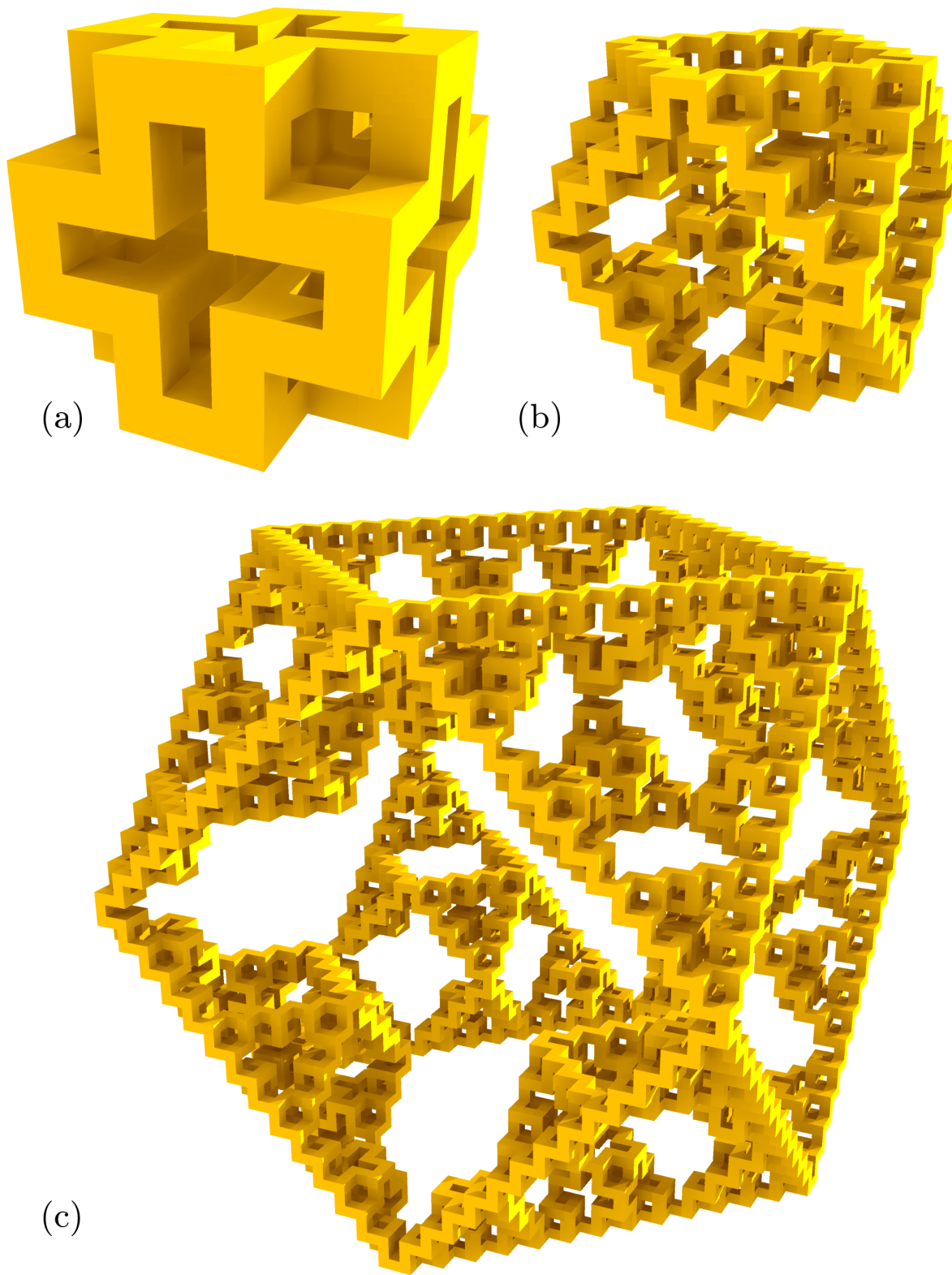


Figure 15. Three stages of the iterated substitution graph following the rules in Figure 14, starting from a cube.

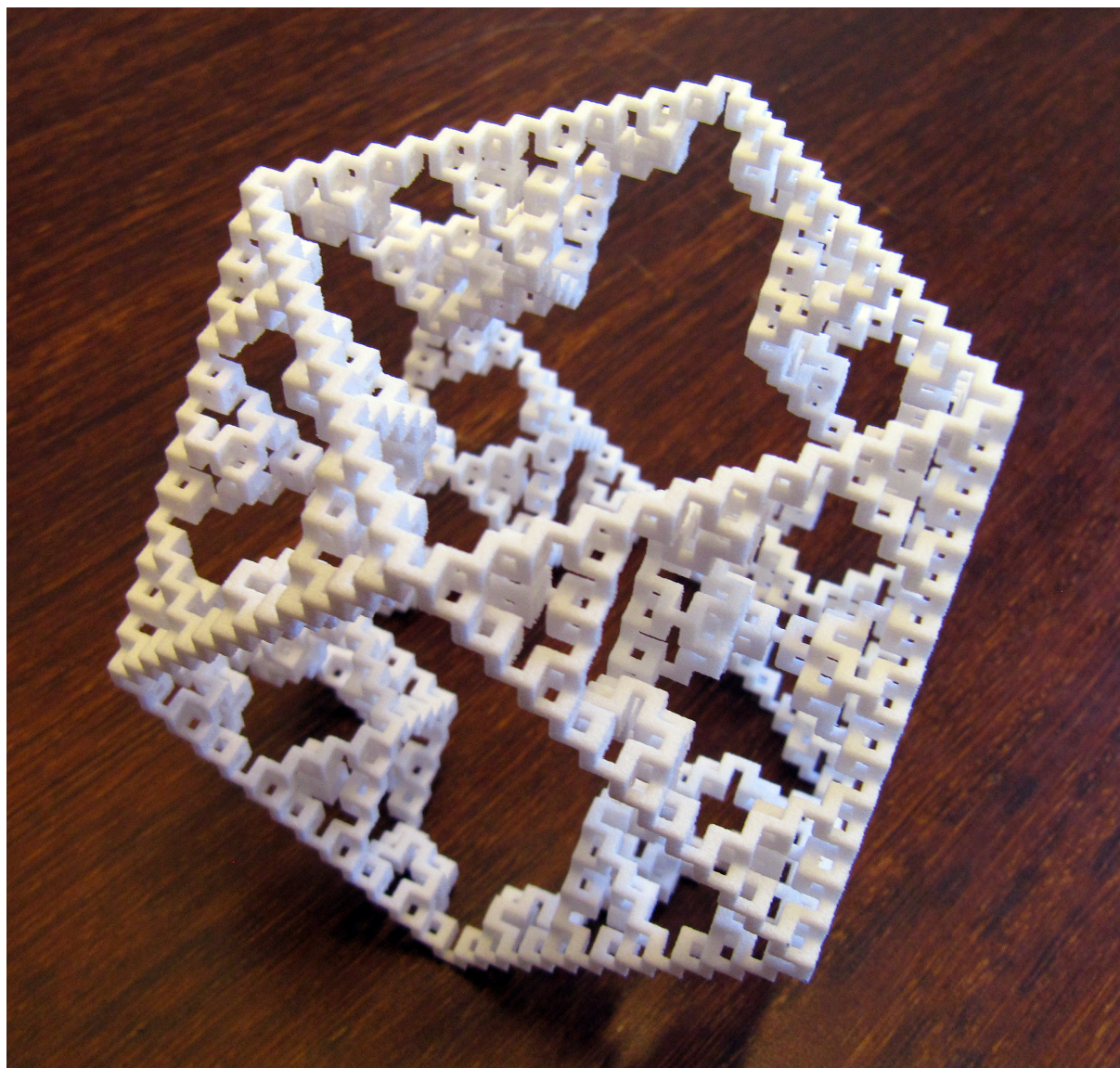


Figure 16. A 3d printed realisation of the lower graph in Figure 15.

We claim that for any given  $v_i$ , if we replace  $A \cap R_{v_i}$  with either  $\emptyset$  or  $R_{v_i}$ , then  $|\partial A|$  either stays the same, or goes down. To see this, first note that there are four possible types of edges connecting from  $R_{v_i}$  to some other  $R_{v_j}$ . Either both ends are in  $A$ , or the  $R_{v_i}$  end is not in  $A$  but the  $R_{v_j}$  end is, or the  $R_{v_i}$  end is in  $A$  but the  $R_{v_j}$  end is not, or neither end is in  $A$ . We denote the numbers of each of these as  $a_a, a_b, b_a$  and  $b_b$  respectively (the main symbol corresponds to  $R_{v_j}$ , the subscript corresponds to  $R_{v_i}$ ). We also denote by  $c$  the number of boundary edges of  $A$  within  $R_{v_i}$ .

Since the edge replacement multiplicity is 1, we have

$$a_a + a_b + b_a + b_b = D \tag{A1}$$

$A \cap R_{v_i} \subset R_{v_i}$  and  $R_{v_i} \setminus A \subset R_{v_i}$ , so

$$D \leq |\partial(A \cap R_{v_i})| = c + a_a + b_a \tag{A2}$$

$$D \leq |\partial(R_{v_i} \setminus A)| = c + a_b + b_b \tag{A3}$$

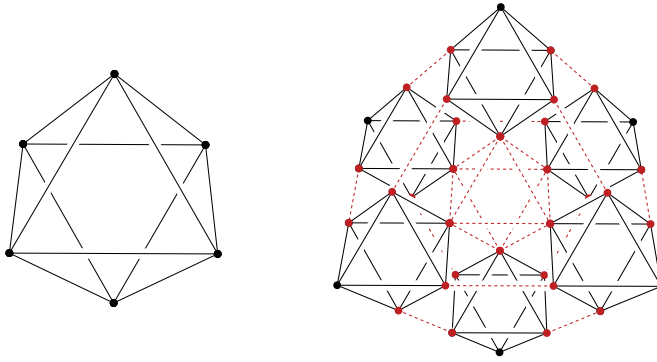


Figure 17. Two stages of the octahedron lattice.

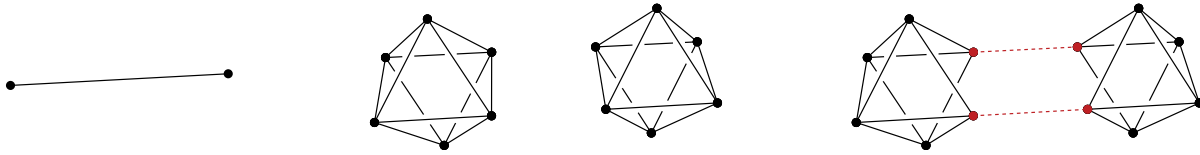


Figure 18. The edge swap move on the octahedron lattice.

The total contribution to  $|\partial A|$  from  $R_{v_i}$  together with the edges from  $R_{v_i}$  to the other  $R_{v_j}$  is  $c + a_b + b_a$ . If we replace  $A \cap R_{v_i}$  with  $\emptyset$  this becomes  $a_a + a_b$ , and if we replace  $A \cap R_{v_i}$  with  $R_{v_i}$  then this becomes  $b_a + b_b$ , so we need to show that  $a_a + a_b \leq c + a_b + b_a$  and  $b_a + b_b \leq c + a_b + b_a$ . Substituting (A1) into (A2) we get:

$$0 \leq c - a_b - b_b \tag{A4}$$

so

$$b_a + b_b \leq c + a_b - b_a \leq c + a_b + b_a \tag{A5}$$

This shows the second desired inequality. The first comes from substituting (A1) into (A3). Thus we can replace all the partial  $A \cap R_{v_i}$  with either  $\emptyset$  or  $R_{v_i}$ , one by one, and each time  $|\partial A|$  either stays the same, or goes down. In order to have  $\frac{|\partial A|}{|A|}$  stay the same or go down, by the end we require that  $|A| = \frac{|V|}{2}$ , which was the maximum value that the original  $|A|$  could take on. Since the number of vertices in  $F_1$  is even there will be an even number of the  $R_{v_i}$ , and we can choose which way to change each partial  $A \cap R_{v_i}$  so that eventually half are in  $A$  and half are not.  $\square$

*Proof* [Proof of Theorem 4.4] Assuming Lemma A.1, note that for the given  $A$ ,  $\frac{|\partial A|}{|A|} = \frac{|\partial A'|}{|A'|} \frac{1}{N_V}$ , where  $A' = \{v \in V_{F_{n-1}} \mid R_v \subset A\}$  (here  $V_{F_{n-1}}$  is the vertex set of  $F_{n-1}$ ), and so to minimise  $\frac{|\partial A|}{|A|}$ , we need to minimise  $\frac{|\partial A'|}{|A'|}$ . By induction, the Cheeger constant is achieved by taking a subset  $A_0$  of the base graph  $F_1$  that achieves its Cheeger constant, then building the subset of  $F_n$  from the descendants of  $A_0$ .  $\square$

*Proof* [Proof of Proposition 4.5] This follows from Theorem 3 of [2] by Bollobás and Leader, which states (in our terminology and for this case) that for any subset  $A$  of the vertices  $V$  of  $C_N$  with  $|A| \leq \frac{N^3}{2}$  that

$$|\partial A| \geq \min_{r=1,2,3} \left\{ |A|^{1-1/r} r N^{(3/r)-1} \right\}$$

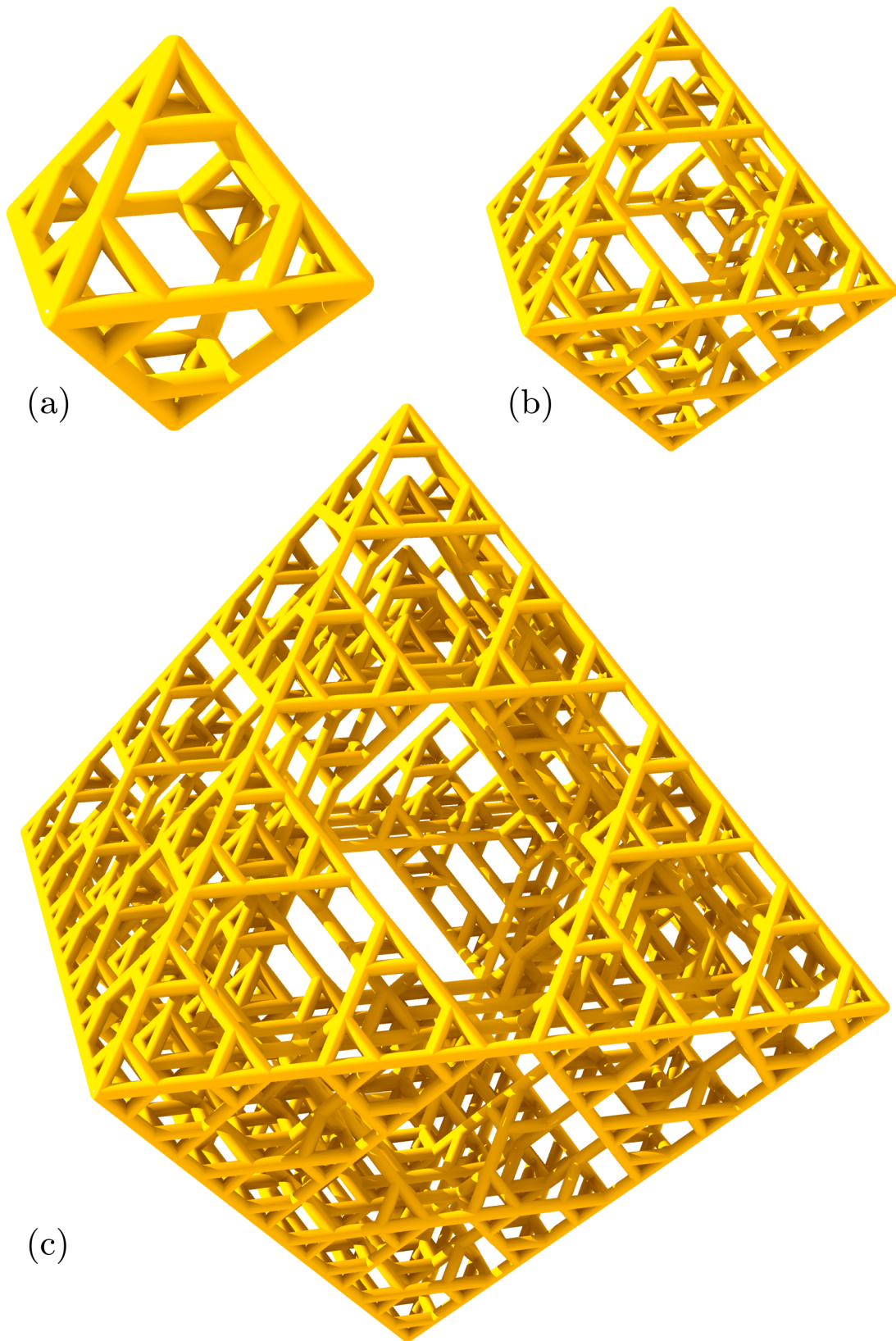


Figure 19. Three stages of an iterated substitution graph on an octahedral lattice, with degree 4 and edge replacement multiplicity 2, constructed by using the edge swap move.

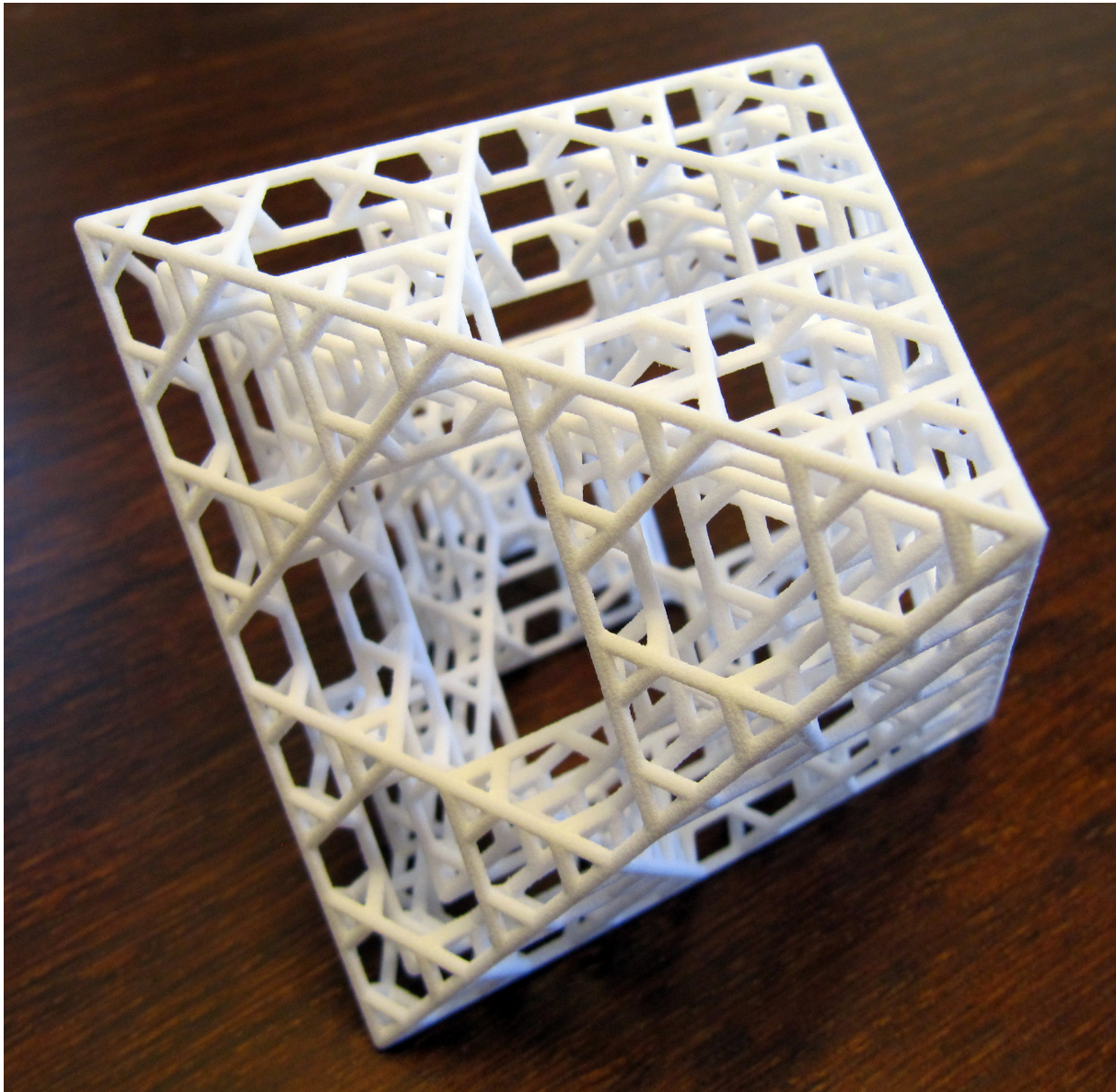


Figure 20. A 3d printed realisation of the lower graph in Figure 19.

So:

$$\min_{r=1,2,3} \left\{ \left( \frac{N^3}{|A|} \right)^{1/r} r \frac{1}{N} \right\} \leq \frac{|\partial A|}{|A|}$$

Now we use:

$$\begin{aligned} |A| &\leq \frac{N^3}{2} \\ 2 &\leq \frac{N^3}{|A|} \\ \frac{r2^{1/r}}{N} &\leq \left( \frac{N^3}{|A|} \right)^{1/r} r \frac{1}{N} \end{aligned}$$

We can check for  $r = 1, 2, 3$  that  $2 \leq r2^{1/r}$ , so we get that

$$\frac{2}{N} \leq \left( \frac{N^3}{|A|} \right)^{1/r} r \frac{1}{N}$$

for each  $r$ , and therefore for the minimum, and so the “orthogonal half” subset of the cube,  $(1, 2, \dots, N/2) \times (1, 2, \dots, N) \times (1, 2, \dots, N)$  which gives  $\frac{|\partial A|}{|A|} = \frac{N^2}{N^3/2} = \frac{2}{N}$ , is best possible.  $\square$